Distribution of diverse nitrogen fixers in the global ocean

F. M. Monteiro,[1,2] M. J. Follows,[1] and S. Dutkiewicz[1]

Received 25 November 2009; revised 23 April 2010; accepted 26 May 2010; published 10 September 2010.

[1] We employ a global three-dimensional model to simulate diverse phytoplanktonic diazotrophs (nitrogen fixers) in the oceans. In the model, the structure of the marine phytoplankton community self-assembles from a large number of potentially viable physiologies. Amongst them, analogs of *Trichodesmium*, unicellular diazotrophs and diatom-diazotroph associations (DDA) are successful and abundant. The simulated biogeography and nitrogen fixation rates of the modeled diazotrophs compare favorably with a compilation of published observations, which includes both traditional and molecular measurements of abundance and activity of marine diazotrophs. In the model, the diazotroph analogs occupy warm subtropical and tropical waters, with higher concentrations and nitrogen fixation rates in the tropical Atlantic Ocean and the Arabian Sea/Northern Indian Ocean, and lower values in the tropical and subtropical South Pacific Ocean. The three main diazotroph types typically co-exist in the model, although *Trichodesmium* analogs dominate the diazotroph population in much of the North and tropical Atlantic Ocean and the Arabian Sea, while unicellular-diazotroph analogs dominate in the South Atlantic, Pacific and Indian oceans. This pattern reflects the relative degree of nutrient limitation by iron or phosphorus. The model suggests in addition that unicellular diazotrophs could add as much new nitrogen to the global ocean as *Trichodesmium*.

Citation: Monteiro, F. M., M. J. Follows, and S. Dutkiewicz (2010), Distribution of diverse nitrogen fixers in the global ocean, *Global Biogeochem. Cycles*, *24*, GB3017, doi:10.1029/2009GB003731.

1. Introduction

[2] Nitrogen fixers or diazotrophs, organisms that fix nitrogen gas (N_2) into organic form, play an important role in the climate system as the availability of inorganic nitrogen can represent a significant limiting factor for marine primary production [*Falkowski et al.*, 1998]. On the global scale, diazotrophy is the largest source of fixed nitrogen in the modern ocean [*Galloway et al.*, 2004; *Gruber*, 2004], counterbalancing the sinks due to denitrification [*Gruber and Sarmiento*, 1997; *Codispoti et al.*, 2001] and anammox [*Devol*, 2003]. It can also have important local consequences: In the oligotrophic North Pacific Ocean, nitrogen fixation is estimated to fuel up to 50% of the new production [*Karl et al.*, 1997].

[3] Diazotrophs in the ocean are represented by a variety of autotrophic and heterotrophic organisms. The diazotrophic heterotrophic community is still poorly understood [*Zehr et al.*, 2000; *Langlois et al.*, 2005], so we focus here on the autotrophs. Three broad categories of marine diazotrophs are associated with photo-autotrophy, which are the cyanobacteria *Trichodesmium* [*Carpenter and Romans*, 1991; *Capone et al.*, 1997; *Karl et al.*, 2002; *LaRoche and Breitbarth*, 2005], unicellular cyanobacteria [*Zehr et al.*, 2001], and symbiotic diazotrophs associated with diatoms [*Carpenter et al.*, 1999; *Foster and Zehr*, 2006].

[4] Much of the current understanding of marine nitrogen fixation comes from the study of *Trichodesmium*; large, filamentous and non-heterocystous cyanobacteria that often aggregate at the surface of the ocean to form colonies. *Trichodesmium* has been observed to grow in most warm oligotrophic subtropical and tropical regions of the ocean [*Carpenter and Romans*, 1991; *Capone et al.*, 1997], apart from the western equatorial and Southeastern subtropical Pacific Ocean [*Mague et al.*, 1974; *Bonnet et al.*, 2008, 2009].

[5] The two other types of marine autotrophic diazotrophs are, as yet, not as well understood. However, it has been suggested that they might add as much new nitrogen to the oceans as *Trichodesmium* [*Carpenter et al.*, 1999; *Zehr et al.*, 2001]. Unicellular diazotrophs were recently discovered by the association of the *nifH* gene, encoding for the nitrogen-fixing enzyme nitrogenase, with small cells [*Zehr et al.*, 1998]. Unicellular diazotrophs are between 10 to 1000 times smaller than *Trichodesmium* (less than 10 μm; *Goebel et al.* [2007]) but have been observed to have nitrogen fixation rates of similar magnitude to that of *Trichodesmium* in the tropical North Atlantic Ocean [*Falcon et al.*, 2004]. Observations indicate the presence of unicellular diazotrophs

[1]Department of Earth, Atmospheric and Planetary Sciences, Massachusetts Institute of Technology, Cambridge, Massachusetts, USA.
[2]School of Geographical Sciences, University of Bristol, Bristol, UK.

0886-6236/10/2009GB003731

in subtropical and tropical waters of the Atlantic Ocean [*Zehr et al.*, 1998; *Falcon et al.*, 2002, 2004; *Montoya et al.*, 2007; *Langlois et al.*, 2008; *Foster et al.*, 2009] and Pacific Ocean [*Zehr et al.*, 2001; *Montoya et al.*, 2004; *Church et al.*, 2005; *Goebel et al.*, 2007; *Bonnet et al.*, 2008; *Church et al.*, 2008], as well as the Arabian Sea [*Mazard et al.*, 2004].

[6] Both *Trichodesmium* and unicellular diazotrophs have been observed to have a relatively low maximum growth rate, high N:P and Fe:P ratios, and to be adapted to high light conditions and warm temperatures [*Falcon et al.*, 2005; *LaRoche and Breitbarth*, 2005; *Goebel et al.*, 2008]. These characteristics are probably related to the high energetic cost of breaking down the N_2 triple bond using the enzyme nitrogenase.

[7] Diatom-diazotroph associations (DDA) have been observed in the ocean for some decades though they are still not well understood due to the complexity of the symbiotic relationship [*Zehr and Ward*, 2002]. Observed DDAs are mostly between *Richelia intracellularis* autotroph diazotrophs and *Hemiaulus hauckii* or *Rhizosolenia clevei* diatoms [*Venrick*, 1974; *Villareal*, 1991; *Carpenter et al.*, 1999; *Gomez et al.*, 2005; *Foster et al.*, 2007]. Observations indicate the presence of DDAs in the tropical and subtropical North Pacific Ocean [*Venrick*, 1974; *Gomez et al.*, 2005; *Church et al.*, 2008; *Kitajima et al.*, 2009], the equatorial North Atlantic Ocean (in particular in the vicinity of the Amazon River plume) [*Villareal*, 1991; *Carpenter et al.*, 1999; *Foster and Zehr*, 2006], in the Mediterranean Sea [*Zeev et al.*, 2008] and the China Sea [*Gomez et al.*, 2005].

[8] Ultimately, continued observations are necessary to define global habitats and nitrogen fixing contributions of each type of diazotroph. Models can help to synthesize and extrapolate the existing observations, as well as to explore hypothesized mechanisms of the regulators of community structure and habitat and to evaluate the integrated rate of nitrogen fixation in the global ocean. However, representing the diverse populations of marine microorganisms in models remains a challenge. Several published models include specific representations of a diazotrophic functional group [e.g., *Fennel et al.*, 2002; *Hood et al.*, 2004; *Moore and Doney*, 2007], typically based on physiological understanding of *Trichodesmium*. For the first time, *Goebel et al.* [2007] resolved multiple diazotrophic types in a model, evaluating nitrogen fixation rates based on *nifH* observations of three diazotroph types (*Trichodesmium* and unicellular Groups A and B), in a one-dimensional representation of station ALOHA in the subtropical North Pacific Ocean.

[9] Here we introduce diazotrophy as a possible physiological function, associated with a variety of other characteristics, into a three-dimensional ocean circulation, biogeochemistry and ecosystem model in which the photo-autotroph communities "self-assemble" from a broad range of initialized phytoplankton types according to their relative fitness in the modeled environment [*Follows et al.*, 2007]. In previous studies, this approach successfully reproduced the distribution of the diverse community of the cyanobacterium *Prochlorococcus* in the Atlantic Ocean [*Follows et al.*, 2007], a plausible biogeography of the dominant functional groups of phytoplankton in the global ocean [*Dutkiewicz et al.*, 2009], as well as the latitudinal gradient in marine phytoplankton diversity [*Barton et al.*, 2010], though diazotrophy was not previously represented.

[10] We first describe the physical, biogeochemical, and ecosystem model (section 2). Then, in order to evaluate the veracity of the modeled plankton communities and nitrogen fixation rates, we compile and compare published direct observations of biomass and nitrogen fixation rates for *Trichodesmium*, unicellular diazotrophs and diatom-diazotroph associations (section 3). We subsequently show that the model system exhibits plausible patterns of abundance and nitrogen fixation rates for the main phytoplanktonic diazotrophs (section 4). This work provides a first cut at a global synthesis of the likely distributions and contributions in fixing nitrogen of three of the main types of marine diazotrophs.

[11] This study focuses on describing the model diazotroph biogeography in the light of a compilation of published observations of diazotroph biomass and nitrogen fixation rates. A deeper investigation into the ecological controls on the emergent model ecosystem is too extensive to include in this manuscript but is the subject of a companion paper (F. M. Monteiro et al., Biogeographical controls on the marine nitrogen fixers, submitted to *Global Biogeochemical Cycles*, 2010).

2. Model Description

[12] Our modeling framework is based on that of *Follows et al.* [2007] and *Dutkiewicz et al.* [2009], where a three-dimensional global ocean model underpins biogeochemical and ecosystem model components with "self-assembling" phytoplankton community structure.

2.1. Ocean Circulation and Biogeochemistry Models

[13] The ocean model (MITgcm; *Marshall et al.* [1997]) is configured in a relatively coarse resolution (1° × 1° horizontally; 23 vertical levels), with sub-mesoscale eddy fluxes parameterized following the work of *Gent and McWilliams* [1990] and boundary layer turbulent mixing following that of *Large et al.* [1994]. We use the ECCO-GODAE state estimates [*Wunsch and Heimbach*, 2007] in which the model circulation has been constrained to closely match in situ and remote observations of the physical environment.

[14] The model ocean transports inorganic and organic forms of phosphorus (P), nitrogen (N), iron (Fe) and silica (Si). None of the external sources of these elements (atmospheric, river or sediments) are represented in the model, except for nitrogen fixation (see later) and the atmospheric deposition of iron, using the model estimates made by *Mahowald et al.* [2005]. Here we assume that 0.8% of deposited iron is bioavailable [*Mahowald et al.*, 2009]. The dynamic representation of the marine iron cycle, following *Parekh et al.* [2005], includes complexation with an organic ligand and particulate scavenging. The biogeochemical and biological tracers interact through the formation, transportation and remineralization of organic matter. Photo-autotrophs are assumed to have fixed elemental ratios and may be consumed by two simple grazers while excretion and mortality, from both phytoplankton and zooplankton, transfer organic matter into sinking particulate and dissolved organic detritus pools. Heterotrophic bacteria are not explicitly

represented. Organic detritus is simply respired back to inorganic forms on a fixed timescale.

[15] Here we also include a more detailed representation of the nitrogen cycling, including explicit representation of nitrogen fixation by diazotrophic phytoplankton (see next paragraph). The combined effect of deep denitrification, anammox and (possibly) heterotrophic diazotrophy is represented in the model very simply, by restoring excess nitrate towards the observed climatology from the World Ocean Atlas 2005 [*Garcia et al.*, 2006] below 200 m depth (details in Appendix A).

2.2. Ecosystem Model

[16] As in the study of *Follows et al.* [2007], we initialize many tens (here 78) of physiologically unique phytoplankton types with characteristics randomly generated from plausible ranges of possible physiologies. The randomization places the organism in one of two nominal size classes ("large" or "small") and assigns parameters regulating the sensitivity of growth to light, nutrients and temperature (Appendix A). Trade-offs are imposed for several characteristics as a function of size: small phytoplankton are presumed to be more efficient at taking up nutrients in oligotrophic conditions, to be able to cope with lower light (due to a lack of package effect), but to be more likely to become photoinhibited and to have slower maximum growth rates. Though, in a general sense growth rate might be expected to decrease with cell size, taxonomic differences can dominate, as seen when comparing laboratory cultures of small, pico-cyanobacteria *Prochlorococcus* and fast-growing, populations of larger diatom cells [*Sarthou et al.*, 2005]. The high maximum growth rates observed for diatoms may in part reflect an enhanced internal store, which can be larger for bigger cell types [*Droop*, 1983] though not accounted for explicitly in our model. The model also randomly selects for the nutrient strategy of the phytoplankton types. For example, a "coin-flip" determines whether a cell type requires silicon; if so it is assumed to be a diatom analog. The rate of change of the biomass of each phytoplankton is determined as a combination of growth (which is a function of light, temperature and nutrient resources), sinking, grazing, mortality and transport by the fluid environment (see *Dutkiewicz et al.* [2009] for full prognostic equations).

[17] Here, we introduce to this framework the possibility for phytoplankton to fix nitrogen gas (N_2). Diazotrophy is also assigned at random and may be associated with any other set of physiological characteristics. The diazotrophs are then assumed to be nitrogen non-limited, to have a smaller specific maximum growth rate (high energetic cost of nitrogen fixing) and higher elemental N:P and Fe:P ratios (high iron requirements of nitrogenase enzyme) than non-diazotrophic phytoplankton (Appendix A). We nominally assume generated diazotrophic cells in the large size class which are not diatoms, to be analogs of *Trichodesmium*; model diatoms which can fix N_2 to be analogs of diatom-diazotroph associations (DDA); and small size-class cells which can fix nitrogen to be analogs of unicellular, cyanobacterial nitrogen fixers. In all simulations presented here, each of these three main diazotroph types is composed of several (typically 3 to 4) phytoplankton types, which differ slightly in physiology. Here we focus on the total population of each main diazotroph type (e.g. *Trichodesmium*), that is the sum of any generated phytoplankton that fall into that classification.

[18] As in our previous studies [*Follows et al.*, 2007; *Dutkiewicz et al.*, 2009], two size classes of grazers are represented in the model, where small (or big) size class preferentially eats small (or big) phytoplankton. For simplicity, here we choose not to have different palatability for the diazotrophs. Though it is probable that *Trichodesmium* has lower grazing pressure than other phytoplankton [*Capone et al.*, 1997], there is evidence that at least one copepod group feeds on *Trichodesmium* [*O'Neil and Roman*, 1994]. More research on grazing pressure would certainly help us to better shape the trade-offs of diazotroph grazers.

[19] Most simulations were integrated for ten model years, after which time a robust seasonal cycle of productivity and phytoplankton community structure has developed and persists for several decades. Over longer timescales the background nutrient distributions drift slightly, driving minor adjustments in biogeography. One simulation was integrated for 100 years and the biogeography, in particular the diazotroph communities, remained relatively constant for that period. Here, all shown results are annual average of the tenth year of simulation. An ensemble of ten simulations was performed, each identical except for the randomization of physiological traits in the initialized organisms. The collection of the ten simulations is the "ensemble" and the individual simulations are the "ensemble members". The biogeographical patterns that are established in the ensemble members were robust and broadly consistent and here we present the "ensemble mean"; the average of the results from the ten simulations.

[20] The resulting biogeography of the main phytoplankton functional groups is very similar to those found in the studies of *Follows et al.* [2007] and *Dutkiewicz et al.* [2009]. Here the model additionally resolves multiple diazotroph types. Though typically at relatively low abundance relative to the main contributors to biomass, the model diazotrophs have a robust distribution which we compare to a compilation of published observations in the following sections.

3. Observations of Diazotroph Biogeography and Nitrogen Fixation

[21] Diazotroph abundance and nitrogen fixation rates have been observed in the ocean for more than 35 years, with early studies related to *Trichodesmium* [*Dugdale et al.*, 1964] and DDAs [*Mague et al.*, 1974]. Published data on the distribution of *Trichodesmium* have been compiled for the global ocean [*Carpenter*, 1983] and the North Atlantic Ocean [*Hood et al.*, 2004]. Here we extend these two compilations to include most currently available observations of occurrence, biomass and nitrogen fixation rates for the three main phytoplanktonic diazotroph types and for the global ocean.

[22] For diazotroph abundance, we compile traditional observations of *Trichodesmium* and DDA (net tow combined with microscopy), video plankton recorder observations of *Trichodesmium* and evaluations of the abundance of

the *nifH* gene for *Trichodesmium*, unicellular diazotrophs and DDAs. Measurement of nitrogen fixation rates comes from acetylene reduction assay or isotopic $^{15}N_2$ methods which have been used to evaluate areal rates (molN m^{-2} d^{-1}) for *Trichodesmium*, unicellular diazotrophs and DDAs. (Some additional published measurements of nitrogen fixation rates are not included here as they integrate the contribution of diazotrophic heterotrophic bacteria which are not represented in the model.)

[23] To compare model results with these observations, we convert the published values into common units (μmolP l^{-1} for diazotroph biomass and μmolN m^{-2} d^{-1} for nitrogen fixation rates) and include both the original measurement and estimated conversion in tabular form in the auxiliary material (Tables S1–S8).[1] The tabulated values include both the uncertainty of the conversion factor and that of the original measurement (e.g. for nitrogen fixation rates, the depth distribution of the diazotroph and the time period of fixation used in the calculation can lead to uncertainties [*Lipschultz and Owens*, 1996]). Here we outline the method of conversion used for the abundance of each diazotroph type.

3.1. *Trichodesmium*

[24] By far the majority of observations on marine nitrogen fixation have been related to *Trichodesmium*. We convert observations of *Trichodesmium* abundances from filaments, cells, colonies or *nifH* copies into units of phosphorus biomass (μmolP l^{-1}). To do so, we use average values of field and laboratory measurements of the amount of phosphorus present in the observed entity (see Text S1 and Tables S1 and S2). The resulting compilation shows that *Trichodesmium* observations (Tables 1 and 2) have relatively good coverage in the North Atlantic Ocean, North East subtropical Pacific Ocean and China Sea, but are more sparse in central South Atlantic Ocean, tropical East Pacific Ocean, middle West subtropical Pacific Ocean and East Indian Ocean.

3.2. Unicellular Cyanobacteria Diazotrophs

[25] Measurements of the abundance of unicellular cyanobacteria diazotrophs in the ocean are made using *nifH* gene sequencing methods. Here we convert the number of *nifH* copies into biomass units (μmolP l^{-1}) for unicellular GroupsA and B by assuming 1 *nifH* copy per cell [*Goebel et al.*, 2007]. Following *Goebel et al.* [2008], since there are no direct measurements of the phosphorus quota in unicellular diazotrophs, we scale *Trichodesmium* phosphorus conversions to the unicellular diazotroph volume, using the allometric relationship for marine phytoplankton developed by *Verity et al.* [1992] (see auxiliary material, Text S1). This scaling introduces some additional uncertainty.

[26] *Goebel et al.* [2007] estimated cell volumes of *Trichodesmium*, unicellular Group B and Group A to be between 200–1000 μm^3, 4–270 μm^3, and 0.2–4.0 μm^3 respectively. Unicellular Group B cell volume is therefore on average two orders of magnitude larger than for unicellular Group A. We sum Group A and Group B biomass to estimate the total populations of unicellulars (Table 3). In most observations of unicellular diazotrophs, *nifH* concentrations are higher for unicellular Group A than for unicellular Group B (see Tables S4 and S5). However the biomass of Group B is generally greater than for unicellular Group A due to the difference in cell volume, thus suggesting a greater contribution to global nitrogen fixation from Group B. Current observations of unicellular diazotrophs in the ocean are mostly restricted to the North Atlantic region, the East subtropical Pacific Ocean and the Arabian Sea (Tables 3 and 4).

3.3. Diatom-Diazotroph Associations

[27] Due to the complexity of symbiotic organisms, the understanding of diatom-diazotroph associations (DDA) remains limited. Detection of DDAs in the ocean relies on specific microscopy (transmitted light and epi-fluorescent) [*Carpenter et al.*, 1999] and *nifH* gene sequencing [*Foster and Zehr*, 2006]. Since no calibration of DDA *nifH* copies to biomass is available, we do not attempt in this study to compare quantities of abundance between the model and the data, but simply make the distinction between presence or absence of DDAs (Table 5, completed by the sparse observations of DDA nitrogen fixation rate in Table 6). We note though that the model itself provides biomass values for the DDA analogs, presented in Figure 1d.

[28] In the following section we present the model results of the abundance and nitrogen fixing activity of the three major marine photo-autotrophic diazotroph types and compare with the compiled observations for occurrence, biomass and nitrogen fixation rates.

4. Model Results: Diazotroph Biogeography and Nitrogen Fixation

[29] Figure 1 presents the ensemble-average, annual mean biomass (μmolP l^{-1}) of the total diazotrophs, *Trichodesmium*, unicellulars, and DDAs in the surface waters (0–50 m) for the tenth year of the ensemble simulation. Here we concentrate on the 0–50 m layer as most observations of diazotroph activity are taken in the upper water column. Figure 2 presents the corresponding model result for nitrogen fixation rates (μmolN $m^{-2}d^{-1}$). Concentrations and rates are presented on a log scale, as values span large ranges. The emergent diazotroph biogeography is relatively robust between the ten-ensemble-member simulations, illustrated in Figure 3 which displays the standard deviation, relative to the mean, of the simulation ensemble. (The standard deviation of nitrogen fixation rates is shown in Figure S1). Over the ten simulations, biomass and rates are consistent for total, *Trichodesmium* and unicellular-diazotroph analogs which have a low standard deviation relative to the mean in most regions. However the standard deviation, relative to the mean is high for the DDAs indicating a greater role of the randomization of physiological characteristics in regulating the habitat of this diazotroph type. This reflects, in part, our inability to define clear trade-offs and the likelihood that we have over-simplified this complex symbiotic relationship in the model.

[1] Auxiliary materials are available with the HTML. doi:10.1029/2009GB003731.

Table 1. Comparison Between Model and Observations of Abundance of *Trichodesmium* (μmolP l^{-1}) in the Global Ocean: Biomass of *Trichodesmium*[a]

	Regions	Model (μmolP l^{-1})	Observations (μmolP l^{-1})	References
A	West subtropical North Atlantic	10^{-7}-10^{-4}	10^{-5}-10^{-4}	*Carpenter* [1983], *Carpenter and Romans* [1991], *Orcutt et al.* [2001], *LaRoche and Breitbarth* [2005], *Davis and McGillicuddy* [2006], and *Langlois et al.* [2008]
B	East subtropical North Atlantic	$\leq 10^{-3}$	10^{-5}-10^{-3}	*Tyrrell et al.* [2003], *Davis and McGillicuddy* [2006], and *Langlois et al.* [2008]
C	Gulf of Mexico	10^{-6}-10^{-4}	10^{-3}	*Carpenter* [1983] and *Carpenter and Romans* [1991]
D	Caribbean	10^{-4}-10^{-3}	10^{-3}	*Carpenter and Price* [1977], *Carpenter* [1983], and *Carpenter and Romans* [1991]
E	West tropical North Atlantic	10^{-4}-10^{-3}	10^{-3}-10^{-2}	*Carpenter* [1983], *Carpenter and Romans* [1991], *Capone et al.* [1997], *Carpenter et al.* [2004], *Foster et al.* [2007], and *Langlois et al.* [2008]
F	East tropical North Atlantic	10^{-4}-10^{-3}	10^{-4}-10^{-2}	*Carpenter* [1983], *Vidal et al.* [1999], *Tyrrell et al.* [2003], and *Langlois et al.* [2008]
G	West tropical South Atlantic	10^{-5}-10^{-3}	$\leq 10^{-4}$	*Carpenter* [1983] and *Tyrrell et al.* [2003]
H	East tropical South Atlantic	10^{-6}-10^{-3}	10^{-5}-10^{-3}	*Carpenter* [1983] and *Tyrrell et al.* [2003]
I	West subtropical South Atlantic	10^{-6}-10^{-4}	10^{-6}-10^{-3}	*Carpenter* [1983] and *Tyrrell et al.* [2003]
J	East subtropical South Atlantic	$\leq 10^{-6}$	10^{-6}	*Carpenter* [1983]
K	East subarctic North Pacific	$<10^{-7}$	below detection	*Church et al.* [2008]
L	West subtropical North Pacific	10^{-5}-10^{-4}	10^{-5}-10^{-2}	*Carpenter* [1983], *Chen et al.* [2003], *Kitajima et al.* [2009], and *Shiozaki et al.* [2009]
M	East subtropical North Pacific	10^{-6}-10^{-4}	10^{-5}-10^{-4}	*Carpenter* [1983], *Letelier and Karl* [1996], *Karl et al.* [1997], N. Goebel (unpublished data, 2008), and *Church et al.* [2008]
N	West tropical North Pacific	10^{-6}-10^{-5}	10^{-5}	*Carpenter* [1983] and *Shiozaki et al.* [2009]
O	Central tropical Pacific	$\leq 10^{-6}$	$\leq 10^{-4}$	*Mague et al.* [1974] and *Church et al.* [2008], 20S-8N, first 10 m
P	West Equatorial Pacific (coastal)	$\leq 10^{-5}$	10^{-3}	*Bonnet et al.* [2009]
Q	West Equatorial Pacific (open ocean)	$<10^{-7}$	below detection	*Mague et al.* [1974] and *Bonnet et al.* [2009]
R	West tropical South Pacific (Great Barrier Reef)	$<10^{-7}$	10^{-6}-10^{1}	*Carpenter* [1983] and *LaRoche and Breitbarth* [2005]
S	West tropical South Pacific	$<10^{-7}$	10^{-3}-10^{-1}	*Dupouy et al.* [2000]
T	East subtropical South Pacific	$<10^{-7}$	below detection	*Mague et al.* [1974] and *Bonnet et al.* [2008]
U	China Sea	10^{-4}-10^{-3}	10^{-5}-10^{-3}	*Carpenter* [1983], *Chang et al.* [2000], *Chen et al.* [2003], *Wu et al.* [2003], and *Dong et al.* [2008]
V	Arabian Sea	10^{-3}-10^{-2}	10^{-4}-10^{-3}	*Somasundar et al.* [1990] and *Capone et al.* [1998]
W	West tropical North Indian Ocean	10^{-3}	10^{-3}	*Carpenter* [1983]
X	West tropical South Indian Ocean	10^{-4}-10^{-3}	10^{-6}	*Carpenter* [1983]
Y	West tropical South Indian Ocean (African coast)	10^{-4}-10^{-3}	10^{-2}-10^{-1}	*Carpenter* [1983], *Carpenter and Romans* [1991], *Kromkamp et al.* [1997], and *Lugomela et al.* [2002]
Z	Mediterranean Sea	10^{-4}	10^{-5}	*Carpenter* [1983]

[a]The areas are labeled with letters and are reported in Figure 1b. The conversions used for *Trichodesmium* abundances are: P:col = 3.87×10^{-3} μmolP col^{-1} [*Mague et al.*, 1977], P:fil = 1.65×10^{-5} μmolP fil^{-1} [*Letelier and Karl*, 1996], cell:fil = 76.6 cell fil^{-1} [*Letelier and Karl*, 1996; *Sanudo-Wilhelmy et al.*, 2001; *Carpenter et al.*, 2004; *LaRoche and Breitbarth*, 2005; *Dong et al.*, 2008], and *nifH* copies:cell = 1 [*Goebel et al.*, 2007]. Data are detailed in the auxiliary material (Text S1 and Tables S1 and S2) and values have been rounded.

[30] We discuss now the modeled biogeography of diazotrophs both collectively and as separate types, in comparison with their observed distributions.

4.1. Sum of Diazotrophs

[31] Although there is no explicit demand that modeled diazotroph analogs grow only in warm waters, the total autotrophic diazotroph population occupies warm subtropical and tropical regions of the ocean (Figure 1a), as is generally observed. While some previous models parameterize their diazotrophic functional types to only grow in warm waters [i.e., *Moore et al.*, 2004, 2006; *Breitbarth et al.*, 2007; *Moore and Doney*, 2007] or stratification conditions [*Hood et al.*, 2004], here this feature is an emergent result of the "self-assembling" model communities. Cold-adapted diazotrophs were initialized in the model but were selected against due to other factors. Collectively, the modeled diazotrophs occupy warm subtropical and tropical waters (Figure 1a for biomass and Figure 2a for nitrogen fixation rate), with higher concentrations and nitrogen fixation rates

Table 2. Comparison Between Model and Observations of Nitrogen Fixation Rates of *Trichodesmium* (μmolN m^{-2} d^{-1}) in the Global Ocean: Nitrogen Fixation Rate of *Trichodesmium*[a]

	Regions	Model (μmolN m^{-2} d^{-1})	Observations (μmolN m^{-2} d^{-1})	References
A	West subtropical North Atlantic	10^{-1}-10^{1}	1-10^{1}	*Capone et al.* [1997], *Carpenter and Price* [1977], *Lipschultz and Owens* [1996], *Orcutt et al.* [2001], and *Davis and McGillicuddy* [2006]
B	East subtropical North Atlantic	$\leq 10^{1}$	10^{-1}	*Lipschultz and Owens* [1996]
D	Caribbean	1-10^{1}	10^{1}-10^{2}	*Carpenter and Price* [1977], *Lipschultz and Owens* [1996], and *Capone et al.* [1997]
E	West tropical North Atlantic	10^{-1}-10^{2}	1-10^{3}	*Capone et al.* [1997], *Carpenter et al.* [1999], *Capone* [2001], *Carpenter et al.* [2004], *Falcon et al.* [2004], *Capone et al.* [2005], *Foster et al.* [2007], and *Montoya et al.* [2007]
F	East tropical North Atlantic	10^{1}-10^{2}	10^{2}	*Montoya et al.* [2007]
M	East subtropical North Pacific	10^{-1}-1	1-10^{2}	*Mague et al.* [1977], *Carpenter* [1983], *Capone et al.* [1997], *Karl et al.* [1997], *Falcon et al.* [2004], *LaRoche and Breitbarth* [2005], *Goebel et al.* [2007], and *Shiozaki et al.* [2009]
O	Central tropical Pacific	$<10^{-2}$	below detection	*Mague et al.* [1974]
S	West tropical South Pacific	$<10^{-2}$	10^{2}	*Garcia et al.* [2007]
U	China Sea	1-10^{2}	10^{1}-10^{2}	*Capone et al.* [1997], *Chang et al.* [2000], *Wu et al.* [2003], and *Dong et al.* [2008]
V	Arabian Sea	10^{1}-10^{2}	10^{1}	*Capone et al.* [1998]
Y	West tropical South Indian Ocean (African coast)	1-10^{1}	10^{3}-10^{4}	*Kromkamp et al.* [1997] and *Lugomela et al.* [2002]

[a]The areas are labeled with letters and are reported in Figure 2b. Data are detailed in the auxiliary material (Text S1 and Table S3) and values have been rounded.

in the tropical Atlantic Ocean, the Arabian Sea, and the Northern Indian Ocean ($\geq 10^{-2}$ μmolP l^{-1} for biomass, and $\geq 10^{2}$ μmolN m^{-2} d^{-1} for nitrogen fixation rates). Much of the central (sub)tropical South Pacific Ocean has very low diazotroph activity. The low iron concentrations there (Figure 5d) and the high requirement for iron imposed on the model diazotrophs limit diazotroph growth in this region of the Pacific Ocean.

4.2. *Trichodesmium* Analogs

[32] The modeled habitat and nitrogen fixation rate of *Trichodesmium* are compared with observations on a regional basis (Tables 1 and 2). Each region is designated by a letter (see Tables 1–6) indicated on the map of *Trichodesmium* surface biomass (Figure 1b) and nitrogen fixation rate (Figure 2b). Both observed and modeled *Trichodesmium* biomass concentration and nitrogen fixation rates

Table 3. Comparison Between Model and Observations of Abundance of Unicellular Diazotrophs (μmolP l^{-1}) in the Global Ocean: Biomass of Unicellular Diazotrophs[a]

	Regions	Model (μmolP l^{-1})	Observations (μmolP l^{-1})	References
a	West subtropical North Atlantic	10^{-5}-10^{-4}	below detection	*Langlois et al.* [2008]
b	East subtropical North Atlantic	10^{-6}-10^{-3}	10^{-5}	*Langlois et al.* [2008]
c	West tropical North Atlantic	10^{-4}-10^{-3}	10^{-5}-10^{-4}	*Foster et al.* [2007] and *Langlois et al.* [2008]
d	East tropical North Atlantic	10^{-4}-10^{-3}	10^{-4}-10^{-3}	*Langlois et al.* [2008] and *Foster et al.* [2009], Gulf of Guinea
e	East tropical South Atlantic	10^{-4}-10^{-3}	10^{-5}	*Foster et al.* [2009], Gulf of Guinea
f	East subarctic North Pacific	$<10^{-7}$	below detection	*Church et al.* [2008]
g	East subarctic/subtropical North Pacific	10^{-7}-10^{-5}	10^{-7}-10^{-5}	*Needoba et al.* [2007] and *Church et al.* [2008]
h	East subtropical North Pacific	10^{-5}-10^{-4}	10^{-5}-10^{-3}	*Church et al.* [2005, 2008], *Goebel et al.* [2007], and *Church et al.* [2009]
i	Central tropical North Pacific	$\leq 10^{-6}$	10^{-6}	*Church et al.* [2008]
j	West Equatorial Pacific	$\leq 10^{-5}$	10^{-7}-10^{-4}	*Church et al.* [2008] and *Bonnet et al.* [2009]
k	East subtropical South Pacific	$<10^{-7}$	below detection	*Bonnet et al.* [2008]
l	26°S 246°	10^{-7}-10^{-6}	10^{-7}	*Bonnet et al.* [2008]
m	Arabian Sea	10^{-3}	10^{-2}	*Mazard et al.* [2004]

[a]The areas are labeled with letters and are reported in Figure 1c. We assume a ratio for *nifH* copies:cell = 1 [*Goebel et al.*, 2007] and use the allometric relationship by *Verity et al.* [1992] to convert phosphorus cell content from *Trichodesmium* estimate to unicellular Groups A and B. Data are detailed in the auxiliary material (Text S1 and Tables S4, S5, and S6) and values have been rounded.

Table 4. Comparison Between Model and Observations of Nitrogen Fixation Rates of Unicellular Diazotrophs (μmolN m^{-2} d^{-1}) in the Global Ocean: Nitrogen Fixation Rate of Unicellular Diazotrophs[a]

	Regions	Model (μmolN m^{-2} d^{-1})	Observations (μmolN m^{-2} d^{-1})	References
a	West subtropical North Atlantic	10^{-1}-10^{1}	1-10^{1}	*Falcon et al.* [2004] and *Foster et al.* [2007]
g	East subarctic/subtropical North Pacific	10^{-2}-10	10^{1}	*Montoya et al.* [2004]
h	East subtropical North Pacific	1-10^{1}	1-10^{2}	*Zehr et al.* [2001], *Falcon et al.* [2004], and *Montoya et al.* [2004]
n	East tropical Indian Ocean (North Australia)	10^{1}	10^{2}	*Montoya et al.* [2004]

[a]The areas are labeled with letters and are reported in Figure 2c. Data are detailed in the auxiliary material (Text S1 and Table S7) and values have been rounded.

vary by an order of magnitude or more even within regions (Tables 1 and 2). The large observed variability within regions may, in part, be due to seasonality, eddies, and sparse sampling.

[33] The large scale patterns in modeled *Trichodesmium* biomass and nitrogen fixation rates is generally consistent with those observed: High *Trichodesmium* concentrations (on the order of 10^{-3} μmolP l^{-1}, equivalent to 10^{4} fil m^{-3}) and nitrogen fixation rates (from 10^{1} to 10^{2} μmolN m^{-2} d^{-1}) occur in the tropical Atlantic Ocean, the Northern Indian Ocean and Arabian Sea. Somewhat lower values are found in the subtropical North Atlantic Ocean (concentrations around 10^{-5} to 10^{-4} μmolP l^{-1} and rates of 10^{1} μmolN m^{-2} d^{-1}). In the subtropical South Atlantic Ocean, model and observations show a sharp gradient in concentrations from about 10^{-4} μmolP l^{-1} in the West, to almost nothing in the East of the basin. Low values characterize most of the North Pacific Ocean in both the model and the observations with about 10^{-5} μmolP l^{-1} of biomass (equivalent to 10^{2} fil m^{-3}) and 1 μmolN m^{-2} d^{-1} of nitrogen fixation rate. Finally the model does not produce any *Trichodesmium* in the East South Pacific: Cruises in this region (Q and T) also did not find any *Trichodesmium* [*Mague et al.*, 1974; *Bonnet et al.*, 2008, 2009].

[34] A few regions in the model have lower biomass of *Trichodesmium* than what is observed. These include the Gulf of Mexico (C), some areas in the Western Pacific Ocean (L, P, R, S) and the Western part of the Indian Ocean (Y). Some of these (C, R, Y) are coastal regimes where tidal mixing, riverine inputs, and other influences unresolved in the model may be important. The modeled Western tropical and subtropical Pacific (L, P, R, S) have very low iron concentrations, potentially due to the lack of parameterization of sediment supply, which might also lead to unrealistically low diazotrophic activity. The Western tropical Indian Ocean (X) and the Mediterranean Sea (Z) have biomass of *Trichodesmium* which are too high in the model. Finally, the modeled nitrogen fixation rates are much lower than observed in the East subtropical North Pacific (M), though the modeled biomass concentrations in the region is similar to the observations. Similarly in the Central tropical Pacific Ocean (region Ø), the model reproduces observations of nitrogen fixation rates but underestimates *Trichodesmium* biomass. These discrepancies between biomass and rate of nitrogen fixers are not understood but might reveal an interesting dynamics present in the real ocean, where *Trichodesmium* fix more (or less) nitrogen than they actually need in the East subtropical North (or Central tropical) Pacific Ocean.

[35] Estimates of the occurrence of *Trichodesmium* blooms based on remote sensing [*Westberry and Siegel*, 2006] found high bloom concentrations in the tropical Atlantic Ocean, the Arabian Sea and the Western Indian Ocean; supporting the modeled distribution presented here. *Westberry and Siegel* [2006] also inferred high *Trichodesmium* concentrations in the Eastern tropical Pacific Ocean consistent with inferences

Table 5. Comparison Between Model and Observations of Occurrence of Diatom-Diazotroph Associations (DDA) in the Global Ocean: Occurrence of Diatom-Diazotroph Associations[a]

	Regions	Model	Observations	References
α	Caribbean	present	present	*Villareal* [1991]
β	West tropical North Atlantic	present	present	*Carpenter et al.* [1999] and *Foster et al.* [2007]
γ	East tropical Atlantic	present	present	*Foster et al.* [2009]
δ	East subarctic North Pacific	none	below detection	*Venrick* [1974] and *Church et al.* [2008]
ε	West subtropical North Pacific	present	present	*Gomez et al.* [2005] and *Kitajima et al.* [2009]
ζ	East subtropical North Pacific	present	present	*Mague et al.* [1974], *Venrick* [1974], and *Church et al.* [2005, 2008, 2009]
η	West tropical North Pacific	present	present	*Kitajima et al.* [2009]
θ	Central tropical North Pacific	none-present	none-present	*Mague et al.* [1974] and *Church et al.* [2008]
ı	West Equatorial Pacific	none	below detection	*Bonnet et al.* [2009]
κ	East South Pacific	none	below detection	*Bonnet et al.* [2008]
λ	26°S 246°	none	present	*Bonnet et al.* [2008]
μ	South China Sea	present	present	*Gomez et al.* [2005]
ν	East Mediterranean Sea	none-present	present	*Zeev et al.* [2008]

[a]The areas are labeled with letters and are reported in Figure 1d.

Table 6. Comparison Between Model and Observations of Nitrogen Fixation Rates of Diatom-Diazotroph Associations in the Global Ocean (μmolN m^{-2} d^{-1}): Nitrogen Fixation Rate of Diatom-Diazotroph Associations[a]

	Regions	Model (μmolN m^{-2} d^{-1})	Observations (μmolN m^{-2} d^{-1})	References
β	West tropical North Atlantic	10^{-1}-10	10^{3}	*Carpenter et al.* [1999]
ζ	East subtropical North Pacific	$\leq$1	10^{1}	*Mague et al.* [1974] and *Carpenter* [1983]
η	West tropical North Pacific	10^{-2}-10^{-1}	10^{2}	*Foster et al.* [2007] and *Kitajima et al.* [2009]
θ	Central tropical North Pacific	$<10^{-2}$	below detection	*Mague et al.* [1974]
ν	East Mediterranean Sea	$\leq10^{-2}$	10^{2}	*Zeev et al.* [2008]

[a]The areas are labeled with letters and are reported in Figure 2d. Data are detailed in the auxiliary material (Text S1 and Table S8) and values have been rounded.

based on geochemical diagnostics [*Deutsch et al.*, 2007]. Here, however, our model solutions show almost no presence of *Trichodesmium*. It is difficult to reconcile the results of both studies by *Deutsch et al.* [2007] and *Westberry and Siegel* [2006] to the direct in situ observations, as so far very little autotrophic diazotrophy has been observed in these regions [*Mague et al.*, 1974; *Bonnet et al.*, 2008, 2009], and seems to support our model solutions.

[36] The model captures the seasonal cycle of *Trichodesmium* at the Bermuda Atlantic Time-series Station, with a notable late summer bloom (Figure 4, shown here for a single ensemble member). *Trichodesmium* biomass varies between about 2×10^{-5} μmolP l^{-1} in the late Spring to about 13×10^{-5} μmolP l^{-1} in the late summer, consistent with time-series observations [*Orcutt et al.*, 2001]. The model predicts a similar, late summer bloom of *Trichodesmium* in the subtropical North Pacific Ocean, as observed at the Hawaii Ocean Time-Series [*Goebel et al.*, 2007; *Church et al.*, 2009]. Here though the seasonality is captured, the modeled abundances are gradually drifting due to a long term trend in the modeled iron concentrations in this region.

4.3. Unicellular Diazotroph Analogs

[37] Both model and observations suggest high concentrations of unicellulars (about 10^{-3} μmolP l^{-1}), with corresponding high nitrogen fixation rates, in most of the East North Atlantic Ocean and Arabian Sea/Indian Ocean (Figure 1c and Table 3 for concentrations, and Figure 2c and Table 4 for rates). Both model and observations suggest lower concentrations and fixation rates in the East subtropical North Pacific (about 10^{-4} μmolP l^{-1} and 10^{1} μmolN m^{-2} d^{-1} respectively) as well as no unicellular diazotroph activity in the East South Pacific, except for a small area in the middle of the subtropical gyre.

[38] The model and observations only differ significantly in the Western subtropical North Atlantic Ocean (A). Here however, the observations provide a mixed perspective with a measured rate of nitrogen fixation of the same order of magnitude as in the North Pacific [*Falcon et al.*, 2004; *Foster et al.*, 2007], consistent with the model solution. In contrast, another cruise found no evidence of unicellular diazotroph abundance from *nifH* analysis [*Langlois et al.*, 2005], whereas the model supports a population of unicellular diazotrophs in agreement with the modeled fixation rate.

[39] Here we treat Group A and Group B both as strict autotrophs. However recent discoveries about the physiology of unicellular Group A indicate that they must rely on organic carbon as they lack the PSII oxygenic photosynthetic apparatus [*Zehr et al.*, 2008] and may participate in a symbiotic relationship [*Tripp et al.*, 2010]. In the current model, we do not clearly represent Group A and their rather special physiology and ecology. As understanding increases, future models may need to treat these organisms differently, with potentially significant implications for overall nitrogen fixation rates.

4.4. Diatom-Diazotroph Association Analogs

[40] Since we are unable to convert the biomass observations of DDAs to model units, we compare patterns of presence or absence of the organisms (Figure 1d and Table 5). DDAs have been observed in the Western side of the (sub) tropical North Atlantic Ocean, the Eastern subtropical and Western tropical North Pacific, the Kuroshio current and the Eastern Mediterranean Sea. The model solutions are consistent except in the Eastern subtropical North Pacific and the Mediterranean Sea where there are no model DDAs. In the model, DDAs are most abundant in the Arabian Sea and the Indian Ocean, as well as the west tropical Atlantic Ocean. The nitrogen fixation rates of modeled DDAs are typically too low at any locations for which there are measurements (Figure 2d and Table 6), perhaps indicating that the parameterization of the symbiotic relationship of a DDA is too simplistic.

[41] Overall, the model captures the main features of the observed habitats for the three diazotroph types and is broadly consistent with observed abundances and rates for *Trichodesmium* and unicellular diazotrophs. The model might underestimate nitrogen fixation by DDAs globally and by *Trichodesmium* in areas of the Western Pacific Ocean.

5. Discussion

5.1. Biogeography of Marine Diazotrophs

[42] The three main diazotrophic types co-exist over much of the modeled subtropical ocean (Figure 5a). Unicellular-diazotroph analogs tend to dominate in the model in most of the regions inhabited by diazotrophs (Figure 5b), especially where iron is limiting (Figures 5c and 5d). The lower nutrient half-saturation constant, a consequence of their smaller size, confers in these regions an advantage on the unicellular diazotrophs. Unicellular-diazotroph analogs also dominate the diazotroph population in a small region of the equatorial Atlantic Ocean, which is characterized by low phosphate concentration rather than low iron concentration (Figures 5c and 5e). When the nutrient limitation is lifted,

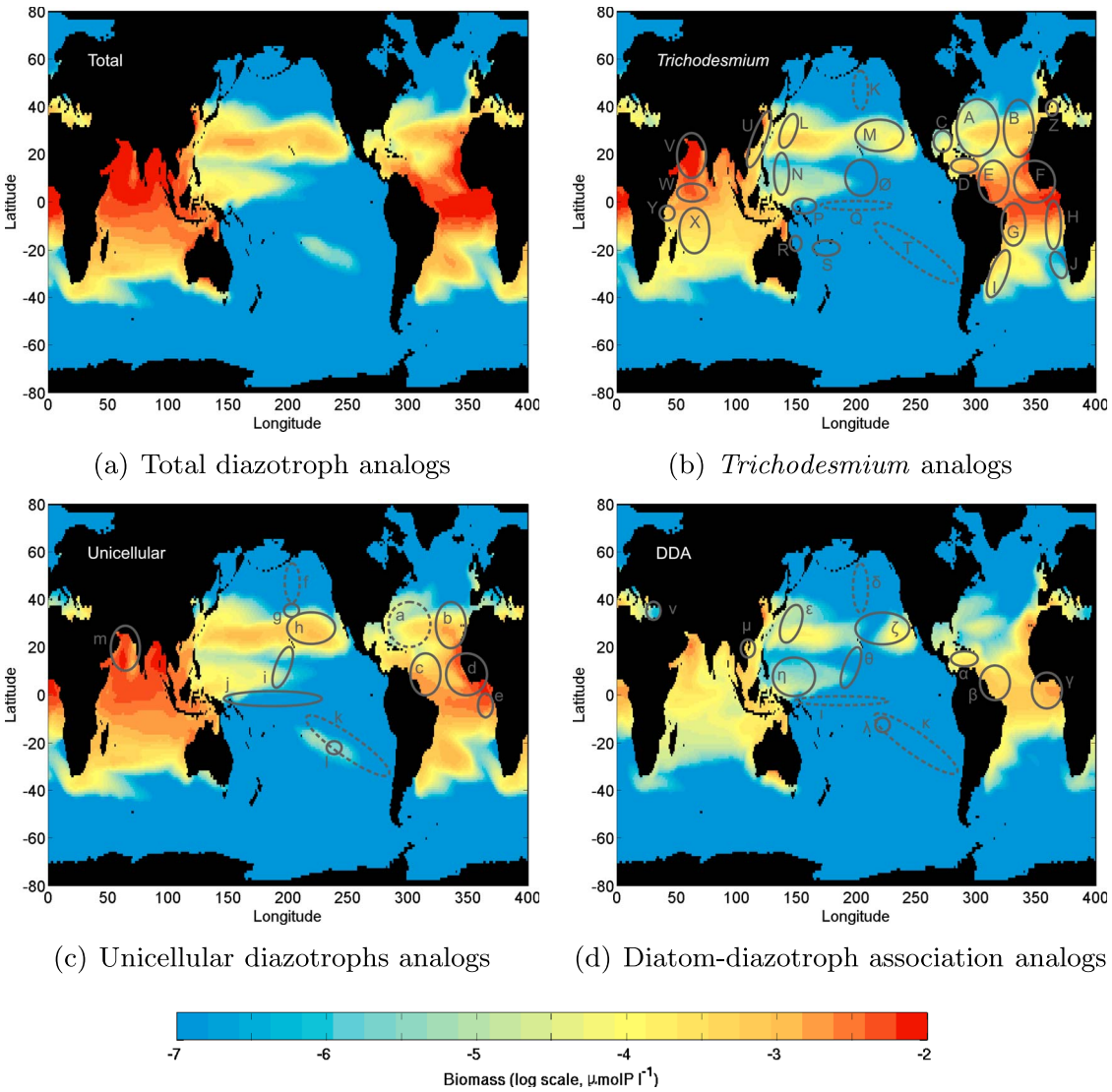

(a) Total diazotroph analogs

(b) *Trichodesmium* analogs

(c) Unicellular diazotrophs analogs

(d) Diatom-diazotroph association analogs

Figure 1. Annual average concentration of diazotroph analogs generated in the model (μmolP l^{-1}, log scale, first 50 m depth) for an ensemble of ten model simulations, each initialized with a different, randomized set of phytoplankton physiologies. Regions of published observations are indicated by letters and ellipses. A solid ellipse denotes observed presence of the organisms of interest. A dashed ellipse denotes that observations were made but the organism of interest was not seen. (a) Total diazotroph abundance. (b) *Trichodesmium* analogs. Letters represent regions with observations of *Trichodesmium* abundance, compared with model results in Table 1. (c) Unicellular-diazotroph analogs. Letters represent regions with observations of unicellular abundance, compared with model results in Table 3. (d) Diatom-diazotroph-association (DDA) analogs. Letters represent regions with observations of DDA occurrence, compared the model results in Table 5.

Trichodesmium analogs are no longer disadvantaged. *Trichodesmium* dominate particularly in regions where iron is more plentiful (subtropical Atlantic Ocean and Arabian Sea). DDAs are found in the model to dominate only in small regions, though we note that the simulated distribution of DDA analogs is quite variable between ensemble members and we are less confident of these predictions.

[43] *Trichodesmium* analogs in our model are responsible for about 43% of the global total nitrogen fixation rate (25 TgN yr^{-1}; section 5.2), while unicellular-diazotroph analogs are responsible for about 49% (30 TgN yr^{-1}) of the global rate. Consistent with previous suggestions [*Carpenter et al.*, 1999; *Zehr et al.*, 2001], our global ocean model explicitly indicates that unicellular diazotrophs could be as important in the global nitrogen budget as *Trichodesmium*. DDA analogs contribute to about 8% of the global nitrogen fixation rate (5 TgN yr^{-1}), though we are not sufficiently comfortable with the parameterization of this symbiotic

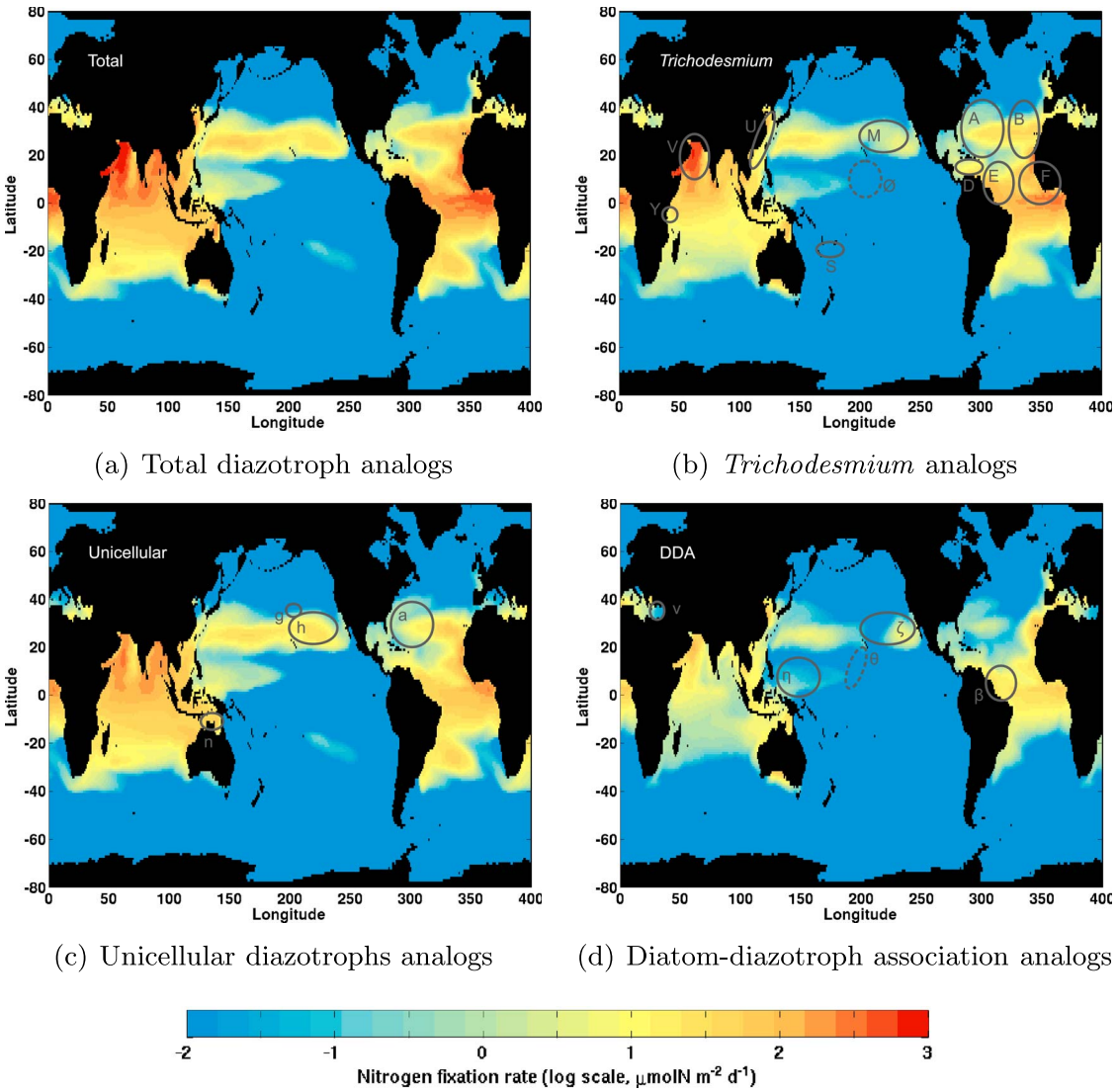

(a) Total diazotroph analogs

(b) *Trichodesmium* analogs

(c) Unicellular diazotrophs analogs

(d) Diatom-diazotroph association analogs

Figure 2. Annual average nitrogen fixation rate of diazotroph analogs generated in the model (μmolN m^{-2} d^{-1}, log scale, first 50 m depth) for an ensemble of ten model simulations, each initialized with a different, randomized set of phytoplankton physiologies. Regions of published observations are indicated by letters and ellipses. A solid ellipse denotes observed rates of the organisms of interest. A dashed ellipse denotes that observations were made but rates of the organism of interestwere undetectable. (a) Total diazotrophs, representing a global nitrogen fixation average of 60 TgN yr^{-1}. (b) *Trichodesmium* analogs, representing 43% of global nitrogen fixation rate. Letters correspond to regions with observations of *Trichodesmium* rates, compared with the model results in Table 2. (c) Unicellular-diazotroph analogs, fixing 49% of the global nitrogen fixation rate. Letters represent regions with observations of unicellular diazotroph rates, comparedwith the model results in Table 4. (d) Diatom-diazotroph-association (DDA) analogs, fixing 8% of the global nitrogen fixation rate. Letters represent regions with observations of DDA rates, compared with the model results in Table 6.

relationship and the robustness of their distribution in the ensemble to be confident of this result.

5.2. Nitrogen Fixation Rates

[44] The global nitrogen fixation rate of our ensemble average is 60 ± 15 TgN yr^{-1} (where the uncertainty is the standard deviation of the ten ensemble members), within the range of published direct and indirect estimates, which vary from 5 to 135 TgN yr^{-1}.

[45] Direct in situ biological estimates increased from early estimates of 5–10 TgN yr^{-1} [*Capone and Carpenter*, 1982; *Carpenter et al.*, 1992] to more recent estimates of

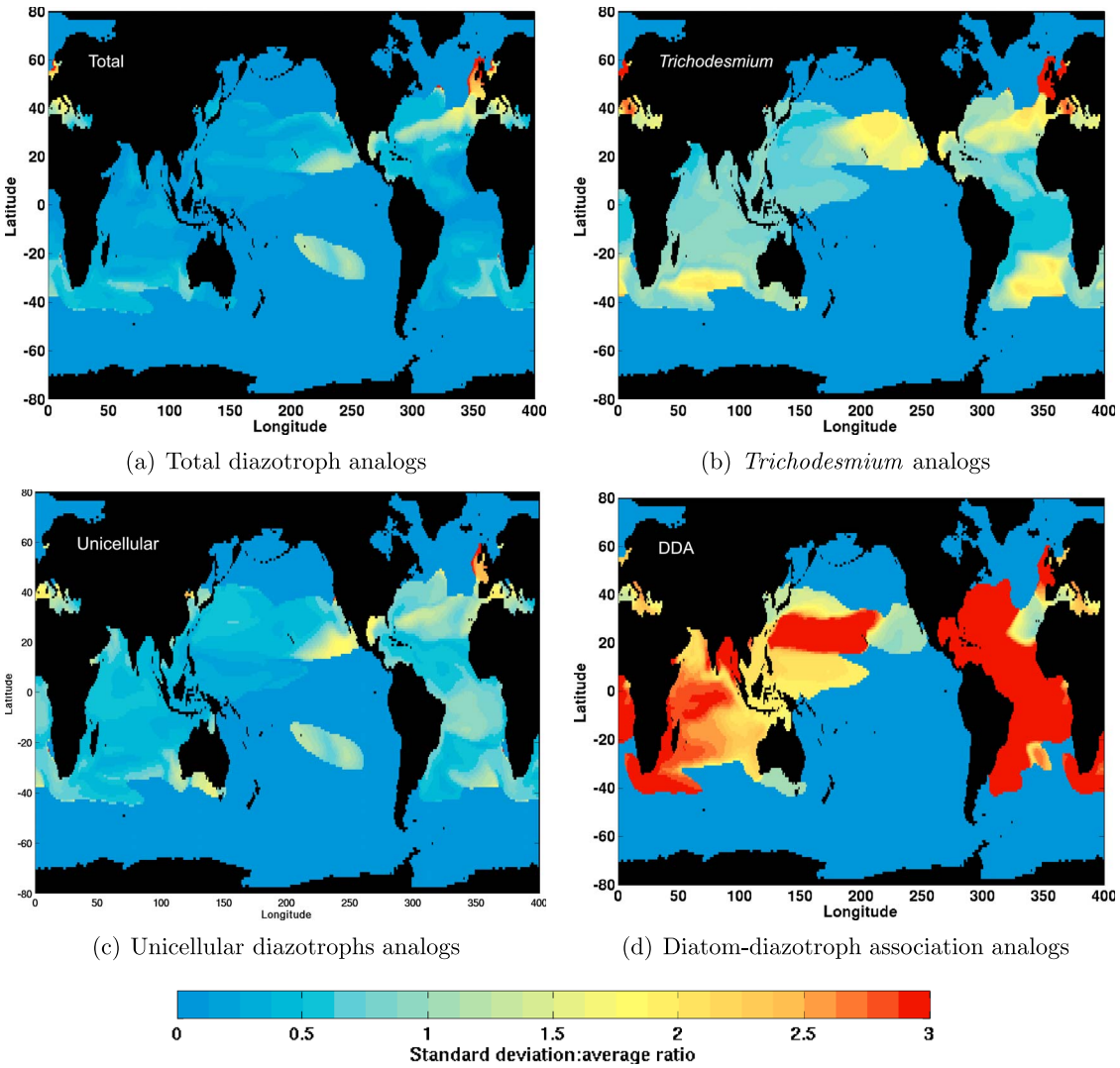

(a) Total diazotroph analogs

(b) *Trichodesmium* analogs

(c) Unicellular diazotrophs analogs

(d) Diatom-diazotroph association analogs

Figure 3. Ratio of the standard deviation over the average of the annual concentration of diazotroph analogs generated in the model for the ten ensemble simulations (no unit, first 50 m depth). (a) Total diazotroph. (b) *Trichodesmium* analogs. (c) Unicellular-diazotroph analogs. (d) Diatom-diazotroph-association (DDA) analogs.

80–85 TgN yr^{-1} [*Capone et al.*, 1997; *Galloway et al.*, 2004]. However these have accounted only for the contribution of *Trichodesmium*, extrapolating sparse measurements to a basin scale or global value for warm oligotrophic regions [*Capone et al.*, 1997; *Galloway et al.*, 2004]. Our model results (and we believe the data compilation) suggest that there are large regional variations in nitrogen fixation even in these warm oligotrophic waters. Thus we suggest that direct estimations of *Trichodesmium* activity [*Capone et al.*, 1997; *Galloway et al.*, 2004] extrapolated from a few measurements have large uncertainties. Our model suggests that *Trichodesmium* only contributes 25 TgN yr^{-1}, though we underestimate *Trichodesmium* nitrogen fixation rates in the Western Pacific Ocean (where iron limitation is too strong) and in coastal zones.

[46] Geochemically based estimates of nitrogen fixation, relying on interpretations of N* and DIN_{xs}, reflect contributions from the entire diazotrophic community (including heterotrophic nitrogen fixers). Geochemical estimates range between 110 and 135 TgN yr^{-1} globally, subject to significant uncertainties [*Gruber and Sarmiento*, 1997; *Gruber*, 2004; *Hansell et al.*, 2004; *Landolfi et al.*, 2008; *Deutsch et al.*, 2007]. The difference with our model result might be in part due to the activity of diazotrophic heterotrophic bacteria which is not resolved here.

[47] Published biogeochemical models have estimated global nitrogen fixation rates ranging from 55 to 100 TgN yr^{-1} [*Moore et al.*, 2002, 2004, 2006] with a clear relationship between rate of iron supply to surface ocean and global nitrogen fixation. Increasing dust-borne iron solu-

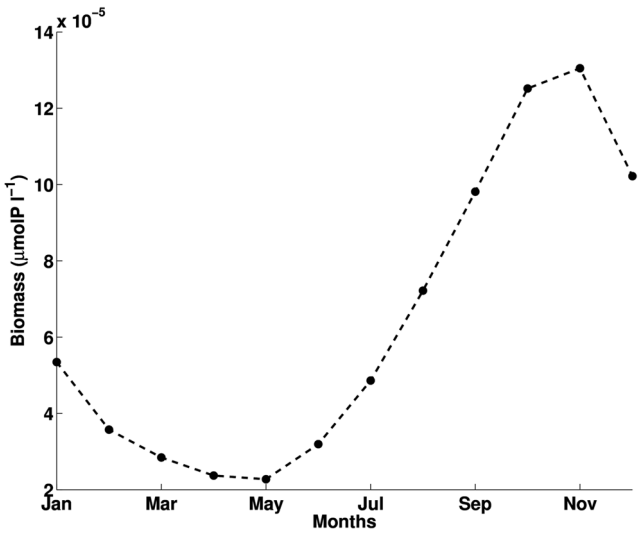

Figure 4. Modeled seasonal variations of *Trichodesmium* biomass (μmolP l^{-1}) at station BATS (31.5°N, 295°W) for a single ensemble member.

bility to 4% in our model induces a global nitrogen fixation rate of 80 ± 30 TgN yr^{-1} but at the expense of fidelity in comparison to the observed data of diazotroph activity. The distribution of the combined diazotroph types in this model is similar to that in previous model studies [*Moore et al.*, 2004; *Moore and Doney*, 2007], which represented a single, generic marine diazotroph based on *Trichodesmium*. Therefore it is possible that the first order global biogeochemical impact of autotrophic nitrogen fixers in the ocean can be captured without the level of diversity modeled in this study. The degree of nitrogen fixation may be rather dictated by the relative shortfall of nutrients (e.g. the available amount of iron and phosphate to the diazotrophs). However the spatial extent of the diazotroph habitat, the stability of the biogeochemical nitrogen system and response to variability and climatic changes are probably all affected by the level of the captured ecological resolution.

[48] The ensemble-mean nitrogen fixation rate over the North Atlantic basin (0°–60°N; 285°W–360°) is 12 ± 4 TgN yr^{-1}. Previous studies have suggested nitrogen fixation rate in the North Atlantic Ocean to vary between 1 and 35 TgN yr^{-1} for direct biological estimates [*Capone and Carpenter*, 1982; *Lipschultz and Owens*, 1996; *Capone et al.*, 2005], between 4 and 85 TgN yr^{-1} for geochemical estimates [*Michaels et al.*, 1996; *Gruber and Sarmiento*, 1997; *Hansell et al.*, 2004; *Deutsch et al.*, 2007; *Hansell et al.*, 2007; *Landolfi et al.*, 2008] and between 8 and 30 TgN yr^{-1} for model estimates [*Coles et al.*, 2004]. Though the North Atlantic Ocean is the most studied region for nitrogen fixation, the large range of estimates indicates the uncertainties associated with all these techniques. The latest and most accurate geochemical study by *Landolfi et al.* [2008] estimated nitrogen fixation rate for the North Atlantic region of 15 TgN yr^{-1}, which is within the standard deviation range of our model ensemble values.

6. Concluding Remarks

[49] We coupled a three-dimensional ocean model with a biogeochemical and ecosystem parameterization to simulate the diverse population of diazotrophic phytoplankton in the global ocean. In this "self-assembling" ecosystem model, analogs of *Trichodesmium*, unicellular diazotrophs and diatom-diazotroph associations (DDA) are enabled and are successful and abundant in each of the ten members of the ensemble of simulations. In addition, we compiled currently available observations of biomass and nitrogen fixation rates for *Trichodesmium*, unicellular diazotrophs and DDAs in order to evaluate the veracity of the model solutions.

[50] The simulations capture the broad character of the observed distribution of *Trichodesmium*, unicellular diazotrophs and DDAs, as well as the abundances and nitrogen fixation rates of *Trichodesmium* and unicellular diazotrophs. They suggest that the three main types of photo-autotrophic diazotrophs co-exist over most of the warm subtropical and tropical waters of the ocean with higher abundances and rates in the tropical North Atlantic Ocean and the Northern Indian Ocean, consistent with the data compilation, diagnostic studies and other models. In this model, the confinement of diazotrophs to warm oligotrophic waters is not imposed but is a result of selection from a broad variety of initialized diazotroph analogs including some adapted to cold temperatures, suggesting that other factors (resource availability) are more significant in defining the habitat. In the Eastern South Pacific Ocean, the model suggests an absence of diazotrophs attributable to iron limitation. This finding is at odds with some other models and diagnostic studies [*Westberry and Siegel*, 2006; *Deutsch et al.*, 2007] but appears to be supported by observations [*Mague et al.*, 1974; *Bonnet et al.*, 2008, 2009]. Diazotroph activity is underestimated in our model in the Western Pacific Ocean because iron limitation is too strong (perhaps due to a lack of sedimentary input) and in the unresolved coastal zones. Our globally integrated nitrogen fixation rate (60 ± 15 TgN y^{-1}) is about half that estimated by geochemical tracers. This may reflect, in part, the fact that we do not resolve heterotrophic diazotrophs and that some regions are too strongly iron limited. An inclusion of sedimentary iron sources and variable iron solubility may help for the latter issue.

[51] In the model, *Trichodesmium* analogs dominate the total diazotroph population in most of the North and tropical Atlantic Ocean and in the Arabian Sea, whereas unicellular-diazotroph analogs dominate in the South Atlantic, Pacific and Indian oceans where iron or phosphorus are less plentiful. The model predicts in particular a high level of nitrogen fixation by unicellular diazotrophs in the Indian Ocean. Observations are still too sparse to support or refute this result. Finally, the model suggests that unicellular diazotrophs globally contribute to add as much new nitrogen to the ocean as *Trichodesmium*, supporting *Zehr et al.* [2001] hypothesis on the importance of small diazotrophs in the

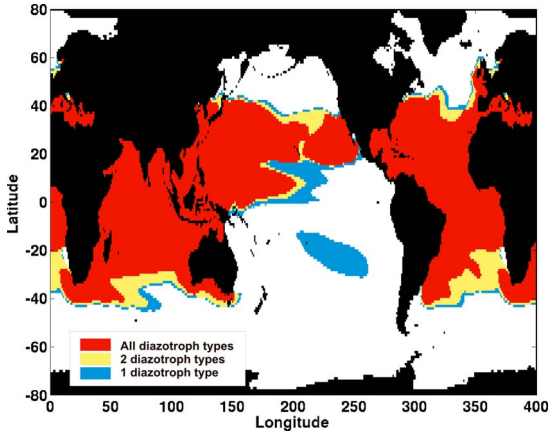

(a) Diversity of diazotroph analogs

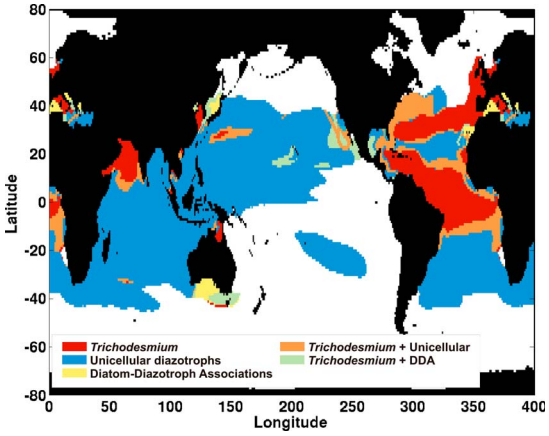

(b) Dominant diazotroph analogs

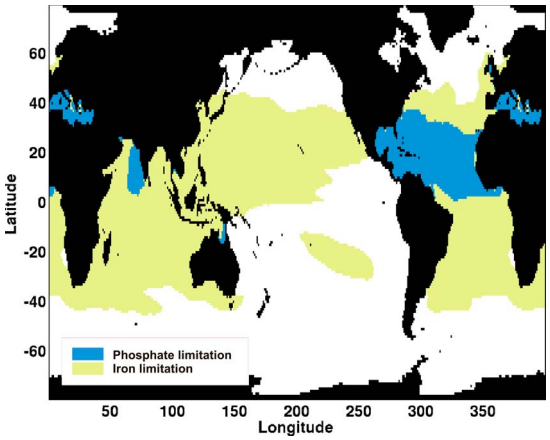

(c) Nutrient limitations of the diazotroph analogs

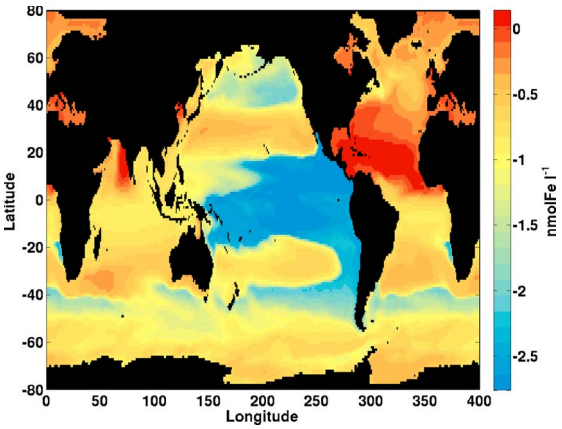

(d) Modeled total iron concentration (nmolFe l^{-1}, log scale) between 0-50 m

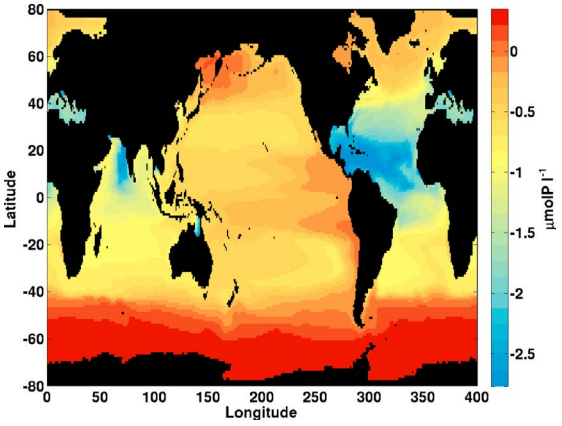

(e) Modeled phosphate concentration (μmolP l^{-1}, log scale) between 0-50 m

Figure 5. Diversity, dominance and nutrient limitations of diazotroph analogs in the model. (a) Diversity of diazotroph analogs (between *Trichodesmium*, unicellular diazotrophs and diatom-diazotroph associations (DDA)). (b) Dominant diazotroph analogs, calculated from the 0–50 m abundance shown in Figure 1. (c) Nutrient limitations between phosphate and iron for the total population of diazotroph analogs. (d) Modeled total iron concentration (nmolFe l^{-1}, log scale) between 0–50 m. (e) Modeled phosphate concentration (μmolP l^{-1}, log scale) between 0–50 m.

marine nitrogen cycle. Thus, while *Trichodesmium* may still be the most observed diazotrophic phytoplankton, any attempt to estimate total global nitrogen fixation rates should include the contribution from other diverse diazotrophic communities. Much remains to be explored as new observations improve our understanding of these different nitrogen fixers and suggest better parameterizations in our model.

Appendix A: Model Ecosystem Parametrization

[52] The ecosystem model equations are similar to that used in the studies of *Follows et al.* [2007] and *Dutkiewicz et al.* [2009]. We use the exact same equations and parameter values as the multiple resource case experiment of *Dutkiewicz et al.* [2009], which are provided in their Appendix. Here we added changes for the nitrogen cycle to include the source of nitrogen fixation and the sink of denitrification (detailed below). We also used a smaller Fe solubility constant (α_{Fe} = 0.008), ideal to represent the distribution of *Trichodesmium* in the North Atlantic Ocean model, and in the range of the observations that vary between 0.01% and 80%, with most values in the lower range [*Mahowald et al.*, 2009].

A1. Nitrogen Fixation

[53] Nitrogen fixation in our model is represented by several autotrophic diazotroph types. When a phytoplankton is generated to be a diazotroph (*Diaz*), we assume the growth to be nitrogen non-limited and to have a smaller maximum growth rate ($\mu_{\max}^{Diaz}$ = 1/2 $\mu_{\max}$) as well as higher N:P and Fe:P elemental ratios (N:P^{Diaz} = 40 mol:mol; Fe:P^{Diaz} = 3 × 10^{-2} mol:mol; see Text S1 in auxiliary material). Sensitivity studies were carried out in the model testing different values of α_{Fe} and Fe:P^{Diaz}: We used those values that provided the best match to the observations of diazotrophs. Diazotroph abundances are observed on average to be ten times smaller that other phytoplankton [*LaRoche and Breitbarth*, 2005]. In our model we initialize diazotroph concentrations to be ten times less than for other phytoplankton; this avoids a large, unrealistic spike of new nitrogen at the beginning of the simulation and therefore reduces the computational time to reach steady state. In addition, we assume a half-saturation constant for unicellular-diazotroph analogs to vary between 0.012 and 0.017 μmolP l^{-1}, which is between the range of *Prochlorococcus* analogs and other small organisms (such as *Synechococcus*). This is because we assume the half-saturation constant to be size-dependent and that unicellular diazotrophs are smaller than most small phytoplankton, and slightly bigger than *Prochlorococcus*.

A2. Nitrate Restoring Scheme

[54] We restore in the model the concentrations of nitrate to the observations (World Ocean Atlas 2005, *Garcia et al.* [2006]) everywhere below 200 m, but only if the concentration exceeds the observation. This provides a crude representation of the combined effect of denitrification, anammox and (possibly) heterotrophic nitrogen fixation in the deep ocean. The model expression for the nitrate restoring scheme is equivalent to:

$$\left(\frac{d\mathrm{NO_3^-}}{dt}\right)_{Nrest} = \frac{1}{\tau_{rest}}\left(\mathrm{NO_3^-} - \mathrm{NO_{3obs}^-}\right),$$

$$\forall\ \mathrm{NO_3^-} > \mathrm{NO_{3obs}^-}\ \&\ z > 200\mathrm{m}$$

[55] τ_{rest} is the restoring time scale, set to 1 year for our presented results. Sensitivity studies reveal that varying τ_{rest} from one year to a decade shows very similar distributions of diazotrophs in the global ocean model.

[56] **Acknowledgments.** Thanks to Jon Zehr, Chris Edwards, Nicole Goebel, Rachel Foster, Ed Boyle, and Maureen Coleman for discussions and advice, as well as Raleigh Hood and an anonymous reviewer for their very insightful comments. We thank the many investigators who have contributed to the growing body of observations of marine diazotrophs and nitrogen fixation rates which have been compiled here. This work was supported by the Gordon and Betty Moore Foundation Marine Microbiology Initiative and NASA.

References

Barton, A. D., S. Dutkiewicz, G. Flierl, J. Bragg, and M. J. Follows (2010), Patterns of diversity in marine phytoplankton, *Science*, 327, 1509–1511, doi:10.1126/science.1184961.

Bonnet, S., et al. (2008), Nutrient limitation of primary productivity in the southeast Pacific (BIOSOPE cruise), *Biogeosciences*, *5*, 215–225.

Bonnet, S., I. C. Biegala, P. Dutrieux, L. O. Slemons, and D. G. Douglas (2009), Nitrogen fixation in the western equatorial Pacific: Rates, diazotrophic cyanobacterial size class distribution and biogeochemical significance, *Global Biogeochem. Cycles*, *23*, GB3012, doi:10.1029/2008GB003439.

Breitbarth, E., A. Oschlies, and J. LaRoche (2007), Physiological constraints on the global distribution of *Trichodesmium*: Effect of temperature on diazotrophy, *Biogeosciences*, *4*, 53–61.

Capone, D. G. (2001), Marine nitrogen fixation: What's the fuss?, *Curr. Opin. Microbiol.*, *4*, 341–348.

Capone, D. G., and E. J. Carpenter (1982), Nitrogen fixation in the marine environment, *Science*, *217*, 1140–1142.

Capone, D. G., J. P. Zehr, H. W. Paerl, B. Bergman, and E. J. Carpenter (1997), *Trichodesmium*, a globally significant marine cyanobacterium, *Science*, *276*, 1221–1229.

Capone, D. G., A. Subramaniam, J. P. Montoya, M. Voss, C. Humborg, A. M. Johansen, R. L. Siefert, and E. J. Carpenter (1998), An extensive bloom of the N_2-fixing cyanobacterium *Trichodesmium erythraeum* in the central Arabian Sea, *Mar. Ecol. Prog. Ser.*, *172*, 281–292.

Capone, D. G., J. Burns, J. Montoya, A. Subramaniam, C. Mahaffey, T. Gunderson, A. Michaels, and E. Carpenter (2005), Nitrogen fixation by *Trichodesmium* spp.: An important source of new nitrogen to the tropical and subtropical North Atlantic Ocean, *Global Biogeochem. Cycles*, *19*, GB2024, doi:10.1029/2004GB002331.

Carpenter, E. J. (1983), Nitrogen fixation by marine *Oscillatoria* (Trichodesmium) in the world's oceans, in *Nitrogen in the Marine Environment*, edited by E. J. Carpenter and D. G. Capone, pp. 65–103, Academic, New York.

Carpenter, E. J., and C. C. Price (1977), Nitrogen fixation, distribution, and production of *Oscillatoria* (*Trichodesmium*) spp. in the western Sargasso and Caribbean seas, *Limnol. Oceanogr.*, *22*(1), 60–72.

Carpenter, E. J., and K. Romans (1991), Major role of the cyanobacterium *Trichodesmium* in nutrient cycling in the North Atlantic Ocean, *Science*, *254*, 1356–1358.

Carpenter, E. J., D. G. Capone, and J. G. Rueter (eds.) (1992), *Marine Pelagic Cyanobacteria: Trichodesmium and Other Diazotrophs*, Kluwer Acad., Dordrecht, Netherlands.

Carpenter, E. J., J. P. Montoya, J. Burns, M. R. Mulholland, A. Subramaniam, and D. G. Capone (1999), Extensive bloom of a N_2-fixing diatom/cyanobacterial association in the tropical Atlantic Ocean, *Mar. Ecol. Prog. Ser.*, *185*, 273–283.

Carpenter, E. J., A. Subramaniam, and D. G. Capone (2004), Biomass and primary productivity of the cyanobacterium *Trichodesmium spp.* in the tropical N. Atlantic Ocean, *Deep Sea Res. Part I*, *51*, 173–203.

Chang, J., K.-P. Chiang, and G.-C. Gong (2000), Seasonal variation and cross-shelf distribution of the nitrogen-fixing cyanobacterium, *Trichodesmium*, in southern East China Sea, *Cont. Shelf Res.*, *20*, 479–492.

Chen, Y. L., H.-Y. Chen, and Y.-H. Lin (2003), Distribution and downward flux of *Trichodesmium* in the South China Sea as influenced by the transport from the Kuroshio Current, *Mar. Ecol. Prog. Ser.*, *259*, 47–57.

Church, M. J., B. D. Jenkins, D. M. Karl, and J. P. Zehr (2005), Vertical distributions of nitrogen-fixing phylotypes at Stn ALOHA in the oligotrophic North Pacific Ocean, *Aquat. Microb. Ecol.*, *38*, 3–14.

Church, M. J., K. M. Bjorkman, D. M. Karl, M. A. Saito, and J. P. Zehr (2008), Regional distributions of nitrogen-fixing bacteria in the Pacific Ocean, *Limnol. Oceanogr.*, *53*(1), 63–77.

Church, M. J., C. Mahaffey, R. M. Letelier, R. Lukas, J. P. Zehr, and D. M. Karl (2009), Physical forcing of nitrogen fixation and diazotroph community structure in the North Pacific Subtropical Gyre, *Global Biogeochem. Cycles*, *23*, GB2020, doi:10.1029/2008GB003418.

Codispoti, L., J. Brandes, J. Christensen, A. Devol, S. Naqvi, H. Paerl, and T. Yoshinary (2001), The oceanic fixed nitrogen and nitrous oxide budgets: Moving targets as we enter the anthropocene?, *Sci. Mar.*, *65*, 85–105.

Coles, V. J., R. Hood, M. Pascual, and D. G. Capone (2004), Modeling the impact of *Trichodesmium* and nitrogen fixation in the Atlantic Ocean, *J. Geophys. Res.*, *109*, C06007, doi:10.1029/2002JC001754.

Davis, C. S., and D. J. McGillicuddy (2006), Transatlantic abundance of the N_2-fixing colonial cyanobacterium *Trichodesmium*, *Science*, *312*, 1517–1520.

Deutsch, C., J. L. Sarmiento, D. M. Sigman, N. Gruber, and J. P. Dunne (2007), Spatial coupling of nitrogen inputs and losses in the ocean, *Nature*, *445*, 163–167.

Devol, A. H. (2003), Solution to a marine mystery, *Nature*, *422*, 575–576.

Dong, J., Y. Zhang, Y. Wang, S. Zhang, and H. Wang (2008), Spatial and seasonal variations of cyanobacteria and their nitrogen fixation rates in Sanya Bay, South China Sea, *Sci. Mar.*, *72*(2), 239–251.

Droop, M. (1983), 25 years of algal growth kinetics. A personal view, *Bot. Mar.*, *26*, 99–112.

Dugdale, R. C., J. J. Goering, and J. H. Ryther (1964), High nitrogen fixation rates in the Sargasso Sea and the Arabian Sea, *Limnol. Oceanogr.*, *9*(4), 507–510.

Dupouy, C., J. Neveux, A. Subramaniam, M. R. Mulholland, J. P. Montoya, L. Campbell, D. J. Carpenter, and D. G. Capone (2000), Satellite capture *Trichodesmium* blooms in the southwestern tropical Pacific, *Eos Trans. AGU*, *81*(2), 13–16.

Dutkiewicz, S., M. J. Follows, and J. G. Bragg (2009), Modeling the coupling of ocean ecology and biogeochemistry, *Global Biogeochem. Cycles*, *23*, GB4017, doi:10.1029/2008GB003405.

Falcon, L. I., F. Cipriano, A. Y. Chistoserdov, and E. J. Carpenter (2002), Diversity of diazotrophic unicellular cyanobacteria in the tropical North Atlantic Ocean, *Appl. Environ. Microb.*, *68*(11), 5760–5764.

Falcon, L. I., E. J. Carpenter, F. Cipriano, B. Bergman, and D. G. Capone (2004), N_2 fixation by unicellular bacterioplankton from the Atlantic and Pacific Oceans: Phylogeny and in situ rates, *Appl. Environ. Microb.*, *70*(2), 765–770.

Falcon, L. I., S. Pluvinage, and E. J. Carpenter (2005), Growth kinetics of marine unicellular N_2-fixing cyanobacterial isolates in continuous culture in relation to phosphorus and temperature, *Mar. Ecol. Prog. Ser.*, *285*, 3–9.

Falkowski, P. G., R. T. Barber, and V. Smetacek (1998), Biogeochemical controls and feedbacks on ocean primary production, *Science*, *281*, 200–206.

Fennel, K., Y. H. Spitz, R. M. Letelier, M. R. Abbott, and D. M. Karl (2002), A deterministic model for N_2 fixation at stn. ALOHA in the subtropical North Pacific Ocean, *Deep Sea Res. Part II*, *49*, 149–174.

Follows, M. J., S. Dutkiewicz, S. Grant, and S. W. Chisholm (2007), Emergent biogeography of microbial communities in a model ocean, *Science*, *315*(5820), 1843–1846.

Foster, R. A., and J. P. Zehr (2006), Characterization of diatom-cyanobacteria symbioses on the basis of *nifH*, *hetR* and 16SrRNA sequences, *Environ. Microbiol.*, *8*, 1913–1925.

Foster, R. A., A. Subramaniam, C. Mahaffey, E. J. Carpenter, D. G. Capone, and J. P. Zehr (2007), Influence of the Amazon River plume on distributions of free-living and symbiotic cyanobacteria in the western tropical north Atlantic Ocean, *Limnol. Oceanogr.*, *53*(2), 517–532.

Foster, R. A., A. Subramaniam, and J. P. Zehr (2009), Distribution and activity of diazotrophs in the Eastern Equatorial Atlantic, *Environ. Microbiol.*, *11*(4), 741–750.

Galloway, J. N., et al. (2004), Nitrogen cycles: Past, present, and future, *Biogeochemistry*, *70*, 153–226.

Garcia, H. E., R. A. Locarnini, T. P. Boyer, and J. I. Antonov (2006), World Ocean Atlas 2005, Volume 4: Nutrients (phosphate, nitrate, silicate), *NOAA Atlas NESDIS 64*, edited by S. Levitus, 396 pp., U.S. Gov. Print. Off., Washington, D. C.

Garcia, N., P. Raimbault, and V. Sandroni (2007), Seasonal nitrogen fixation and primary production in the southwest Pacific: Nanoplankton diazotrophy and transfer of nitrogen to picoplankton organisms, *Mar. Ecol. Prog. Ser.*, *343*, 25–33.

Gent, P., and J. McWilliams (1990), Isopycnal mixing in ocean general circulation models, *J. Phys. Oceanogr.*, *20*, 150–155.

Goebel, N., C. A. Edwards, B. J. Carter, K. M. Achilles, and J. P. Zehr (2008), Growth and carbon content of three different-sized diazotrophic cyanobacteria observed in the subtropical North Pacific, *J. Phycol.*, *44*, 1212–1220.

Goebel, N. L., C. A. Edwards, M. J. Church, and J. P. Zehr (2007), Modeled contributions of three types of diazotrophs to nitrogen fixation at station ALOHA, *ISME*, *1*, 606–619.

Gomez, F., K. Furuya, and S. Takeda (2005), Distribution of the cyanobacterium *Richelia intracellularis* as an epiphyte of the diatom *Chaetoceros compressus* in the western Pacific Ocean, *J. Plankton Res.*, *27*(4), 323–330.

Gruber, N. (2004), The dynamics of the marine nitrogen cycle and its influence on atmospheric CO_2 variations, in *The Ocean Carbon Cycle and Climate*, *NATO Sci. Ser. IV*, vol. 40, edited by M. Follows and T. Oguz, pp. 97–148, Kluwer Acad., Dordrecht.

Gruber, N., and J. L. Sarmiento (1997), Global patterns of marine nitrogen fixation and denitrification, *Global Biogeochem. Cycles*, *11*(2), 235–266.

Hansell, D. A., N. R. Bates, and D. B. Olson (2004), Excess nitrate and nitrogen fixation in the North Atlantic Ocean, *Mar. Chem.*, *84*, 243–265.

Hansell, D. A., D. B. Olson, F. Dentener, and L. M. Zamora (2007), Assessment of excess nitrate development in the subtropical North Atlantic, *Mar. Chem.*, *106*, 562–579.

Hood, R. R., V. J. Coles, and D. G. Capone (2004), Modeling the distribution of *Trichodesmium* and nitrogen fixation in the Atlantic Ocean, *J. Geophys. Res.*, *109*, C06006, doi:10.1029/2002JC001753.

Karl, D. M., R. Letelier, J. Dore, J. Christian, and D. Hebel (1997), The role of nitrogen fixation in biogeochemical cycling in the subtropical North Pacific Ocean, *Nature*, *388*, 533–538.

Karl, D. M., et al. (2002), Dinitrogen fixation in the world's oceans, *Biogeochemistry*, *57/58*, 47–98.

Kitajima, S., K. Furuya, F. Hashihama, and S. Takeda (2009), Latitudinal distribution of diazotrophs and their nitrogen fixation in the tropical and subtropical western North Pacific, *Limnol. Oceanogr.*, *54*(2), 537–547.

Kromkamp, J., M. DeBie, N. Goosen, J. Peene, P. VanRijswijk, J. Sinke, and G. C. A. Duineveld (1997), Primary production by phytoplankton along the Kenyan coast during the SE monsoon and November intermonsoon 1992, and the occurrence of *Trichodesmium*, *Deep Sea Res. Part II*, *44*(6–7), 1195–1212.

Landolfi, A., A. Oschlies, and R. Sanders (2008), Organic nutrients and excess nitrogen in the North Atlantic subtropical gyre, *Biogeosciences*, *5*, 1199–1213.

Langlois, R. J., J. LaRoche, and P. A. Raab (2005), Diazotrophic diversity and distribution in the tropical and subtropical Atlantic Ocean, *Appl. Environ. Microb.*, *71*(12), 7910–7919.

Langlois, R. J., D. Hummer, and J. LaRoche (2008), Abundance and distributions of the dominant *nifH* phylotypes in the North Atlantic Ocean, *Appl. Environ. Microb.*, *74*(6), 1922–1931.

Large, W. G., J. C. McWilliams, and S. C. Doney (1994), Oceanic vertical mixing: A review and a model with a nonlocal boundary layer parameterization, *Rev. Geophys.*, *32*(4), 363–403.

LaRoche, J., and E. Breitbarth (2005), Importance of the diazotrophs as a source of new nitrogen in the ocean, *J. Sea Res.*, *53*, 67–91.

Letelier, R. M., and D. M. Karl (1996), Role of *Trichodesmium* in the productivity of the subtropical North Pacific Ocean, *Mar. Ecol. Prog. Ser.*, *133*, 263–273.

Lipschultz, F., and N. J. P. Owens (1996), An assessment of nitrogen fixation as a source of nitrogen to the North Atlantic Ocean, *Biogeochemistry*, *35*, 261–274.

Lugomela, C., T. J. Lyimo, I. Bryceson, A. K. Semesi, and B. Bergman (2002), *Trichodesmium* in coastal waters of Tanzania: diversity, seasonality, nitrogen and carbon fixation, *Hydrobiologia*, *477*, 1–13.

Mague, T. H., N. M. Weare, and O. Holm-Hansen (1974), Nitrogen fixation in the North Pacific Ocean, *Mar. Biol.*, *24*, 109–119.

Mague, T. H., F. C. Mague, and O. Holm-Hansen (1977), Physiology and chemical composition of nitrogen-fixing phytoplankton in the central North Pacific Ocean, *Mar. Biol.*, *41*, 213–227.

Mahowald, N. M., A. R. Baker, G. Bergametti, N. Brooks, R. A. Duce, T. D. Jickells, N. Kubilay, J. M. Prospero, and I. Tegen (2005), Atmospheric global dust cycle and iron inputs to the ocean, *Global Biogeochem. Cycles*, *19*, GB4025, doi:10.1029/2004GB002402.

Mahowald, N. M., et al. (2009), Atmospheric iron deposition: Global distribution, variability, and human perturbations, *Annu. Rev. Mar. Sci.*, *1*, 245–278.

Marshall, J., C. Hill, L. Perelman, and A. Adcroft (1997), Hydrostatic, quasi-hydrostatic and nonhydrostatic ocean modeling, *J. Geophys. Res.*, *102*, 5733–5752.

Mazard, S. L., N. J. Fuller, K. M. Orcutt, O. Bridle, and D. J. Scanlan (2004), PCR analysis of the distribution of unicellular cyanobacterial diazotrophs in the Arabian Sea, *Appl. Environ. Microb.*, *70*(12), 7355–7364.

Michaels, A. F., D. Olson, J. L. Sarmiento, J. W. Ammerman, K. Fanning, R. Jahnke, A. H. Knap, F. Lipschultz, and J. M. Prospero (1996), Inputs, losses and transformations of nitrogen and phosphorus in the pelagic North Atlantic Ocean, *Biogeochemistry*, *35*(1), 181–226.

Montoya, J., C. Holl, J. Zehr, A. Hansen, T. Villareal, and D. Capone (2004), High rates of N_2 fixation by unicellular diazotrophs in the oligotrophic Pacific Ocean, *Nature*, 430.

Montoya, J. P., M. Voss, and D. G. Capone (2007), Spatial variation in N_2-fixation rate and diazotroph activity in the tropical Atlantic, *Biogeosciences*, *4*, 369–376.

Moore, J. K., and S. C. Doney (2007), Iron availability limits the ocean nitrogen inventory stabilizing feedbacks between marine denitrification and nitrogen fixation, *Global Biogeochem. Cycles*, *21*, GB2001, doi:10.1029/2006GB002762.

Moore, J. K., S. C. Doney, D. M. Glover, and I. Y. Fung (2002), Iron cycling and nutrient-limitation patterns in surface waters of the World Ocean, *Deep Sea Res. Part II*, *49*, 463–507.

Moore, J. K., S. C. Doney, and K. Lindsay (2004), Upper ocean ecosystem dynamics and iron cycling in a global three-dimensional model, *Global Biogeochem. Cycles*, *18*, GB4028, doi:10.1029/2004GB002220.

Moore, J. K., S. C. Doney, K. Lindsay, N. Mahowald, and A. F. Michaels (2006), Nitrogen fixation amplifies the ocean biogeochemical response to decadal timescale variations in mineral dust deposition, *Tellus, Ser. B*, *58*, 560–572.

Needoba, J. A., R. A. Foster, C. Sakamoto, J. P. Zehr, and K. S. Johnson (2007), Nitrogen fixation by unicellular diazotrophic cyanobacteria in the temperate oligotrophic North Pacific Ocean, *Limnol. Oceanogr.*, *52*(4), 1317–1327.

O'Neil, J. M., and M. R. Roman (1994), Ingestion of the cyanobacterium *Trichodesmium* spp. by pelagic harpacticoid copepods *Macrosetella*, *Miracia* and *Oculosetella*, *Hydrobiologia*, *292/293*, 235–240.

Orcutt, K., F. Lipschultz, K. Gundersen, R. Arimoto, A. Michaels, A. Knap, and J. Gallon (2001), A seasonal study of the significance of N_2 fixation by *Trichodesmium* spp. at the Bermuda Atlantic Times-series Study (BATS) site, *Deep Sea Res. Pt. II*, *48*, 1583–1608.

Parekh, P., M. J. Follows, and E. A. Boyle (2005), Decoupling of iron and phosphate in the global ocean, *Global Biogeochem. Cycles*, *19*, GB2020, doi:10.1029/2004GB002280.

Sanudo-Wilhelmy, S., et al. (2001), Phosphorus limitation of nitrogen fixation by *Trichodesmium* in the central Atlantic Ocean, *Nature*, *411*, 66–69.

Sarthou, G., K. R. Timmermans, S. Blain, and P. Treguer (2005), Growth physiology and fate of diatoms in the ocean: A review, *J. Sea Res.*, *53*, 25–42.

Shiozaki, T., K. Furuya, T. Kodama, and S. Takeda (2009), Contribution of N_2 fixation to new production in the western North Pacific Ocean along 155°E, *Mar. Ecol. Prog. Ser.*, *377*, 19–32.

Somasundar, K., A. Rajendran, M. D. Kumar, and R. S. Gupta (1990), Carbon and nitrogen budgets of the Arabian Sea, *Mar. Chem.*, *30*, 363–377.

Tripp, H. J., S. R. Bench, K. A. Turk, R. A. Foster, B. A. Desany, F. Niazi, J. P. Affourtit, and J. P. Zehr (2010), Metabolic streamlining in an open-ocean nitrogen-fixing cyanobacterium, *Nature*, *464*, 90–94.

Tyrrell, T., E. Maranon, A. J. Poulton, A. R. Bowie, D. S. Harbour, and E. M. S. Woodward (2003), Large-scale latitudinal distribution of *Trichodesmium* spp. in the Atlantic Ocean, *J. Plankton Res.*, *25*(4), 405–416.

Venrick, E. L. (1974), The distribution and significance of *Richelia intracellularis* Schmidt in the North Pacific central gyre, *Limnol. Oceanogr.*, *19*(3), 437–445.

Verity, P. G., C. Y. Robertson, C. R. Tronzo, M. G. Andrews, J. R. Nelson, and M. E. Sieracki (1992), Relationships between cell-volume and the carbon and nitrogen-content of marine photosynthetic nanoplankton, *Limnol. Oceanogr.*, *37*(7), 1434–1446.

Vidal, M., C. M. Duarte, and S. Agustí (1999), Dissolved organic nitrogen and phosphorus pools and fluxes in the central Atlantic Ocean, *Limnol. Oceanogr.*, *1*, 106–115.

Villareal, T. A. (1991), Nitrogen-fixation by the cyanobacterial symbiont of the diatom genus *Hemiaulus*, *Mar. Ecol. Prog. Ser.*, *11*, 117–132.

Westberry, T. K., and D. A. Siegel (2006), Spatial and temporal distribution of *Trichodesmium* blooms in the world's oceans, *Global Biogeochem. Cycles*, *20*, GB4016, doi:10.1029/2005GB002673.

Wu, J., S.-W. Chung, L.-S. Wen, K.-K. Liu, Y.-L. L. Chen, H.-Y. Chen, and D. M. Karl (2003), Dissolved inorganic phosphorus, dissolved iron, and *Trichodesmium* in the oligotrophic South China Sea, *Global Biogeochem. Cycles*, *17*(1), 1008, doi:10.1029/2002GB001924.

Wunsch, C., and P. Heimbach (2007), Practical global oceanic state estimation, *Phys. D*, *230*, 197–208.

Zeev, E. B., T. Yogev, D. Man-Aharonovich, N. Kress, B. Herut, O. Beja, and I. Berman-Frank (2008), Seasonal dynamics of the endosymbiotic nitrogen-fixing cyanobacterium *Richelia intracellularis* in the eastern Mediterranean Sea, *ISME*, *2*, 911–923.

Zehr, J. P., and B. Ward (2002), Nitrogen cycling in the ocean: New perspectives on processes and paradigms, *Appl. Environ. Microb.*, *68*(3), 1015–1024.

Zehr, J. P., M. T. Mellon, and S. Zani (1998), New nitrogen-fixing microorganisms detected in oligotrophic oceans by amplification of nitrogenase (*nifH*) genes, *Appl. Environ. Microb.*, *64*(9), 3444–3450.

Zehr, J. P., E. Carpenter, and T. Villareal (2000), New perspectives on nitrogen-fixing microorganisms in tropical and subtropical oceans, *Trends Microbiol.*, *8*(2), 68–73.

Zehr, J. P., J. B. Waterbury, P. J. Turner, J. P. Montoya, E. Omoregie, G. F. Steward, A. Hansen, and D. M. Karl (2001), Unicellular cyanobacteria fix N_2 in the subtropical North Pacific Ocean, *Nature*, *412*, 635–638.

Zehr, J. P., S. R. Bench, B. J. Carter, I. Hewson, F. Niazi, T. Shi, H. J. Tripp, and J. P. Affourtit (2008), Globally distributed uncultivated oceanic N_2-fixing cyanobacteria lack oxygenic photosystem II, *Science*, *322*, 1110–1112.

S. Dutkiewicz and M. J. Follows, Department of Earth, Atmospheric and Planetary Sciences, Massachusetts Institute of Technology, 77 Massachusetts Ave., Cambridge, MA 02139, USA.

F. M. Monteiro, School of Geographical Sciences, University of Bristol, University Road, Bristol BS8 1SS, UK. (f.monteiro@bristol.ac.uk)